Tellus (1996), 48B, 445–456
Printed in UK – all rights reserved

TELLUS
ISSN 0280–6509

Longitudinal and vertical CO_2 gradients over the subtropical/subantarctic oceanic sink

By P. MONFRAY[1,*], M. RAMONET[1,2] and D. BEARDSMORE[3] [1]*Centre des Faibles Radioactivités, CNRS/CEA, F91198 Gif sur Yvette, France;* [3]*Division of Atmospheric Research, CSIRO, Private Bag 1, Mordialloc, Victoria 3195, Australia;* [2]*Climate Monitoring and Diagnostics Laboratory, NOAA, Boulder, CO 80303, USA*

(Manuscript received 23 January 1996; in final form 10 June 1996)

ABSTRACT

The North-South gradient of atmospheric CO_2 is commonly used to infer the latitudinal distribution of sources and sinks at the earth surface. Here we analyze the East–West and vertical gradients occurring at regional scale over the subtropical/subantarctic ocean (around 30°S–45°S), which is known to be the major sink of the southern hemisphere. Using French and Australian inter calibrated datasets, we find a significant depletion of atmospheric CO_2 near Tasmania (Cape Grim, 40°41′S, 144°41′E, CGO) compared to the open Indian Ocean (Amsterdam Is., 37°48′S, 77°32′E, AMS). This depletion was about -0.4 ± 0.2 ppmv for the 1988–1992 period. For the same period, CGO values were also depleted by -0.85 ± 0.25 ppmv and -1.1 ± 0.4 ppmv relative to the mid- and high-troposphere. Using a 3-D atmospheric transport model based on meteorological analysis, and a diagnostic CO_2 flux scenario updated for the year 1990, we investigate the respective role of industrial, oceanic and biospheric fluxes. The main component which can explain such longitudinal and vertical oceanic sink appears to be the subtropical/subantarctic oceanic sink and its regional patterns. Using the oceanographic datasets in the Atlantic, Pacific, and West Indian oceans, we can reconstruct more than half of vertical gradient observed over CGO, but not the CGO depletion relative to AMS. Finally, we discuss the hypothesis of an extra oceanic CO_2 sink south of the Australian mainland.

1. Introduction

Atmospheric CO_2 monitoring network has been widely used to infer the latitudinal location and strength of CO_2 sources and sinks (Keeling et al., 1989; Tans et al., 1990; Ciais et al., 1995). Basically, the interhemispheric CO_2 gradient, of the order of 3 ppmv, suggests that major sinks are located in mid latitudes of the both hemispheres. In the southern hemisphere the major sink, whose strength and patterns are still largely unknown, is the Southern Ocean near subtropical/subantarctic zone (Keeling et al., 1989; Tans et al., 1990; Ramonet, 1994). In the present paper, we focus on southern mid-latitudes in order to study how the observed atmospheric gradients can be related to the regional sources and sinks. At these latitudes three stations are monitoring continuously the atmospheric CO_2 concentrations: Amsterdam Island (37°48′S, 77°32′E, AMS), Cape Grim (40°41′S, 144°41′E, CGO) and Baring Head (41°40′S, 174°90′E). An unexpected feature of this regional network is a systematic depletion of CGO relative to the two other stations (Pearman et al., 1991; Enting and Pearman, 1993). Such a depletion, of about 1 ppmv, points out the problem of representing a latitudinal band by only one station. This is a crucial problem for the studies of the global carbon cycle and implies the need for a world wide intercalibrated CO_2 network to establish zonal or regional patterns of CO_2 fluxes.

[1] Corresponding author.

In the following, we present: (1) the French and Australian datasets at AMS, CGO and in the free troposphere, using a common CO_2 scale, (2) the 3-D atmospheric transport model TM2Z, and a new assessment of CO_2 fluxes, (3) the simulated CO_2 gradients taking into account the role of baseline selection, and (4) an analysis of the respective role of fossil fuel CO_2, continental biosphere and ocean in the observed gradients.

2. Atmospheric CO_2 datasets

Atmospheric CO_2 has been continuously monitored at AMS since 1980, and at CGO since 1976, using NDIR analyzer providing a reproducibility better than 0.05 ppmv (Gaudry et al., 1987, 1990; Lambert et al., 1995; Beardsmore and Pearman, 1987). A careful intercalibration of the CO_2 scales used at CGO and AMS was made in August 1990 with an accuracy better than 0.1 ppmv (Monfray et al., 1992). It revealed an offset of the Australian scale in comparison to the French one of -0.6 ppmv. Part of this offset was due to the drift of CO_2 concentrations in three tanks, which were part of a set of 11 WMO standard tanks used to define the Australian scale (Beardsmore and Pearman, 1995). By using only the 8 stable tanks, Bearsdmore (1996) has recalculated the CO_2 concentrations for the period 1987–1992. The above offset between CGO and AMS in 1990 was then reduced to -0.2 ppmv. Hereafter, the CO_2 gradients are corrected for this offset, and so the two stations can be considered as intercalibrated to within 0.1 ppmv for the year 1990.

The monthly differences (CGO minus AMS) of baseline CO_2 concentrations are plotted on Fig. 1a. In addition to the 1990 data we have plotted the 5 years mean and standard deviation, corresponding to the period 1988–1992. This multi-years curve illustrates the climatological mean and the inter-annual variability of the CGO/AMS gradient, around 1990. As is made clear by Fig. 1a, the CGO monthly values are systematically depleted relative to AMS values, except in September. The difference is greater during summertime (January and February). It is worth noting that during the austral summer airmasses arriving at AMS can be originated from the North (Miller et al., 1993), inducing a relative decoupling between AMS and CGO. Within the

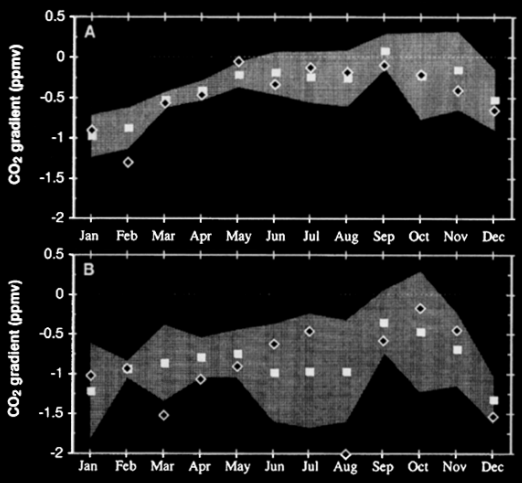

Fig. 1. CO_2 monthly gradients over Austral Indian ocean. The observed differences of CGO relative to AMS (a) and to the mid-troposphere (b) are displayed for 1990 (open diamonds), and for 1988–1992 period (open squares) with standard deviation (shaded area).

1988–1992 period, the annual surface difference CGO minus AMS is -0.4 ± 0.2 ppmv. If we exclude January and February, the average difference is -0.25 ppmv, with a standard deviation of 0.15 ppmv. Such permanent East–West gradients, of a few tenths of ppmv, are a bit surprising due to the strong westerly winds blowing throughout the main part of the year in the Roaring Forties. Furthermore, they are of the same order of magnitude than the North-South gradients in the austral area (Keeling et al., 1989; Tans et al., 1990; Ramonet, 1994).

Another important data set is given by the samples made in the mid-troposphere (at about 4 km height) over Bass Strait and CGO (Pearman and Beardsmore, 1984; Fraser et al., 1992). The air flasks are analyzed at the DAR/CSIRO main laboratory (Aspendale, Australia). Monfray et al. (1992) pointed out an offset of -0.2 ppmv between the DAR/CSIRO main laboratory and the CGO scale. Consequently, the vertical gradients of CO_2 concentration: CGO (continuous analyzer) minus the mid-troposphere (flask sampling), have been corrected by -0.2 ppmv. This is in agreement with the bias (-0.2 ± 0.2 ppmv) found at CGO between surface flask sampling and the continuous analyzer (Beardsmore and Pearman, 1990, 1991, 1992, 1994 and 1995). The corrected vertical gradi-

ents are plotted on Fig. 1b for the year 1990 and the period 1988–1992. A negative value corresponds to a depletion at sea level (i.e. at CGO). Monthly vertical gradients are more scattered than the CGO/AMS gradients due to the low sampling frequency in the mid-troposphere (around six flasks per month), and also because there is no systematic selection for marine conditions. Despite this scattering, it appears that the surface values (CGO) are systematically depleted compared to the mid-troposphere by -0.93 ppmv in 1990, and by around -0.85 ± 0.25 ppmv for the period 1988–1992. The lowest depletion occurs from September to November.

Finally, thanks to automated air samplers mounted in commercial aircraft, DAR/CSIRO has made CO_2 measurements in the high troposphere (at about 9 km height) since 1974 (Pearman and Beardsmore, 1984). Despite the scattering of the observations, due to the sampling over a wide area (the southern part of Australia) and the very low frequency (once or twice a month), the surface data are found to be lower than the high troposphere data: -1.07 ppmv in 1990, and -1.1 ± 0.4 ppmv for the period 1988–1992.

In the following part of the paper, we examine if our present knowledge about the CO_2 fluxes exchanged with the atmosphere can explain the observed vertical and longitudinal gradients.

3. The atmospheric transport model, and CO_2 fluxes for the year 1990

The link between atmospheric gradients and regional distribution of CO_2 fluxes, is achieved through the atmospheric transport. For this purpose we used the 3-D model TM2 developed by Heimann (1995). The advection, vertical diffusion and convection in cumulus are driven with 1990 reconstructed fields of winds, pressure, temperature, humidity and latent heat fluxes from ECMWF. In addition, improvement of the resolution from $10° \times 8°$ to $2.5° \times 2.5°$ had been performed for regional studies (Ramonet et al., 1996). The vertical resolution of the model is 9 iso-sigma layers distributed from the surface to 10 hPa. There is no explicit PBL (planetary boundary layer) in the TM2Z, and tracers emitted at the surface are homogeneously distributed in the first layer (around 400 m). The TM2Z model has been used to simulate the concentrations of Radon-222 (a radioactive continental tracer) both at sea level (Ramonet, 1994) and in the free troposphere (Ramonet et al., 1996).

A new assessment of sources and sinks was also made for the year 1990, following the approach of Heimann and Keeling (1989). The global scenario was split in 10 components: one for the industrial releases; four for the terrestrial biosphere (net primary productivity or NPP, heterotrophic respiration, deforestation, fertilization effect); and five for the oceanic exchanges (North Atlantic, North Pacific, Tropical Oceans, subantarctic/subtropical Oceans and Antarctic Ocean). All of them have been updated to 1990 (Ramonet, 1994). In particular, NPP has been calculated from remote sensing NDVI for the year 1990 (Ruimy et al., 1994). For each of the ten components a 4 years run was performed with a perpetual 1990 meteorology. Simulated atmospheric CO_2 concentrations were extracted each hour during the fourth year.

Because this study is designed as a regional study, focused on the mid-southern latitudes, a special attention was given to the air/sea CO_2 exchanges over the subtropical/subantarctic oceans, i.e. the band between 20°S and the Polar Front ($\approx 50°$S). North of 20°S the space-time distribution of the ΔpCO_2 is similar to the distribution used by Heimann and Keeling (1989). The magnitude of the global CO_2 fluxes in these regions are adjusted in order to obtain the best fit with the annual mean of the latitudinal gradient observed in 1990. South of the Polar Front the ΔpCO_2 is known to be very variable due to the biological activity in the surface water (Inoue et al., 1988; Metzl et al., 1991; Takahashi et al., 1993; Poisson et al., 1993). However, the atmospheric data seem to indicate that there is a CO_2 source in the waters around Antarctica (Tans et al., 1990). Because there is not enough data to estimate the space-time distribution of ΔpCO_2 in this region, we have chosen a constant value of 10 μatm (Tans et al., 1990).

For the oceanic exchanges in the subtropical/subantarctic area, we used new datasets of ΔpCO_2 over the Indian and Atlantic oceans (Poisson et al., 1993; Weiss et al., 1992). These data provided seasonal relationships between ΔpCO_2 and SST (Ramonet, 1994). Then, the oceanic fluxes were calculated from the Liss and Merlivat (1986) relationship by using the surface temperature and

wind fields at 10m given by the ECMWF's analyses for the year 1990. The exchange coefficients were scaled by a factor of 1.77 to get an annual mean of 0.06 mol m^{-2} y^{-2} $ppmv^{-1}$ according to the 14C budget (Broecker et al., 1986). It must be emphasized that we did not adjust the oceanic fluxes deduced from the observed ΔpCO_2 and SST maps in the subantarctic/subtropical region. The annual distribution of ΔpCO_2 is shown in Fig. 2, together with the locations of the oceanographic cruises. It clearly indicates the position of the oceanic CO_2 sink in the subtropical/subantarctic zone (30°S–45°S), estimated around 1.4 ± 1.0 GtC y^{-1} (Ramonet, 1994). The annual CO_2 flux distribution is shown on Fig. 3.

It is well-known that a large inter-annual variability of the latitudinal gradient occurs (Conway et al., 1994; Keeling et al., 1995; Francey et al., 1995) corresponding mainly to change in CO_2 fluxes rather than in atmospheric circulation (Law and Simmonds, 1996; Bousquet et al., 1996). In the subtropical/subantarctic zone, our estimated CO_2 fluxes do not correspond, in the strict sense, to the particular year 1990: ΔpCO_2 are derived from a climatological oceanographic dataset (see above) without adjustment procedure for 1990, while CO_2 gas exchange coefficients are computed for the year 1990. So, in the following, we compare simulated longitudinal and vertical gradient at 40°S both with the 1990 observed values and with the estimated climatological gradients (specifically the range observed during the period 1988–1992).

Using the same transport model and the same flux distribution, an extensive study of the CO_2 seasonal cycle over the Austral Indian ocean had been performed (Ramonet, 1994; Ramonet and Monfray, 1996). These studies demonstrated the ability of the TM2Z to reproduce with a good precision (± 0.3 ppmv) the seasonal cycles observed at the major austral stations. In the following, we analyze the annual gradients simulated by the TM2Z model over the subantarctic/subtropical ocean in terms of fossil fuel, biospheric and oceanic contributions. Also, we compare simulated values to the data.

4. Simulated CO_2 gradients over the Austral Indian ocean

The latitude-height cross section of the CO_2 annual means simulated at the longitude of CGO (144°E) is displayed in Fig. 4. The large interhemispheric gradient (3 ppmv) is mostly induced by the industrial CO_2 released in the northern hemisphere. The southern upper troposphere appears to be relatively rich in CO_2 compared to the lower troposphere. This is due to the fact that: (1) air parcels are transported from one hemisphere into the other predominantly via the upper troposphere

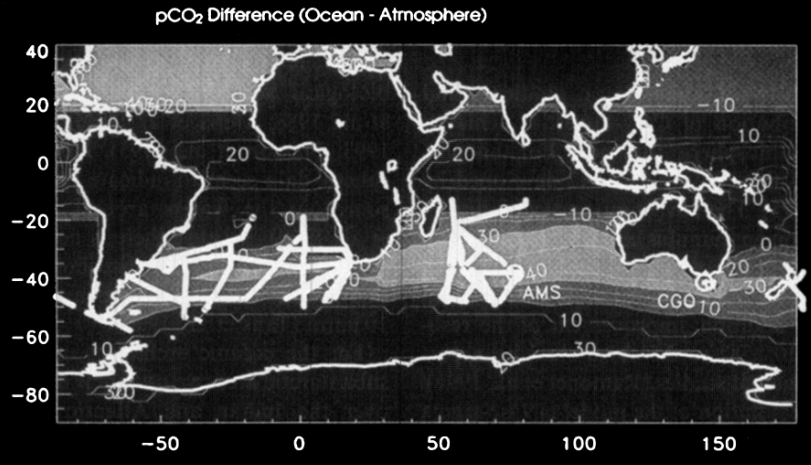

Fig. 2. Annual ΔpCO_2 (ocean–atmosphere) in ppmv. The thick black lines show the oceanographic cruises from which we used the measurements to establish seasonal ΔpCO_2 maps in subtropical/subantarctic area. Isolines are displayed each 10 ppmv from −50 to 50 ppmv. Shaded area corresponds to the negative values, and dark gray to the values lower than −30 ppmv.

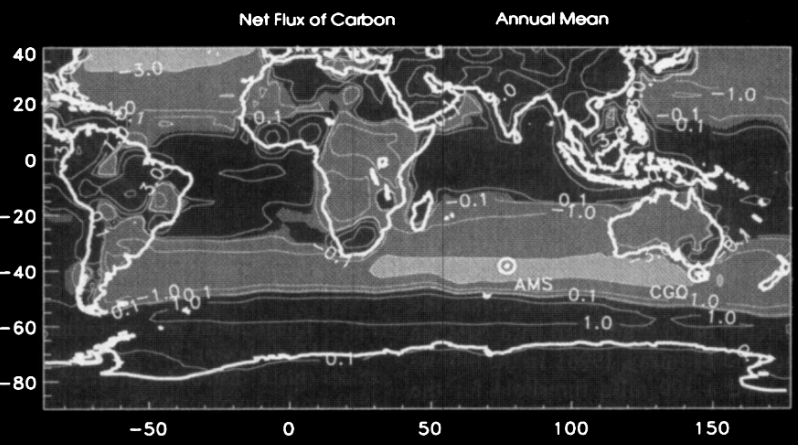

Fig. 3. Annual net flux of carbon for 1990. Isolines are -10, -3, -1, -0.1, 0.1, 1, 3, 10, 100 10^{-2} kgC m^{-2} yr^{-1}. Shaded area corresponds to the negative values (from the atmosphere to the biosphere/oceans), and dark gray to the values lower than -3 10^{-2} kgC m^{-2} yr^{-1}.

Fig. 4. Vertical section of atmospheric CO_2 at 144°E. Values are referred to the South Pole. Isolines are -0.2, 0.0, 0.2, 0.4, 0.6, 0.8 ppmv, and each 0.5 ppmv from 1 to 6 ppmv. Shaded areas correspond to concentrations greater or equal to 1 ppmv.

(Prather et al., 1987; Plumb and Malham, 1987; Taguchi, 1993; Bousquet et al., 1996), and (2) the oceanic surface is a CO_2 sink at mid-southern latitudes (Fig. 3). Finally, over Australia a CO_2 enhancement is found due to nearby fossil fuel emission.

These continental influences are removed from the time series observed at CGO. Indeed, the baseline selection aims to select only periods of long-range transport over the ocean (Beardsmore and Pearman, 1987). It was pointed out by Ramonet and Monfray (1996) that some precautions have to be taken when comparing baseline data, with simulated values in coastal stations like CGO. To take into account the role of baseline selection on surface and free tropospheric simu-

lated values, we have used criteria based on simulated Radon-222, a radioactive continental tracer emitted by soil with a 3.8 d life time. Basically, air masses associated with rich Radon-222 concentration are considered to be recently affected by continental fluxes. Ramonet and Monfray (1996) considered a 500 mBq threshold to select baseline periods at CGO. The value of this threshold can be chosen in a relative wide range but a low value would reject too much data for reliable means (Law, 1996), and a high value would increase the synoptic dispersion in contradiction with baseline data (Ramonet and Monfray, 1996). In the following, we have used a 100 mBq threshold for the whole tropospheric column above CGO. Such a value enables us to obtain similar results to Ramonet and Monfray (1996) who used a 500 mBq threshold (annual mean is changed by only 0.02 ppmv). It also gives a significant rejection ratio (around 0.5) in the free troposphere where Radon-222 values are significantly lower than at the surface (Ramonet et al., 1996; Heimann et al., 1990). Finally, no correction has been made over AMS where the baseline selection affects very slightly the CO_2 cycle because the island is very far from the continents (Ramonet and Monfray, 1996).

The simulated vertical gradient over CGO and AMS are plotted, together with the observations, in Fig. 5. All the values are referred to the annual concentration at CGO taking into account the baseline selection. The CO_2 concentrations simulated in the upper layers above CGO are shown both with and without applying the Radon-222 criteria to select the baseline values. The main feature of the vertical gradients is an increase of CO_2 concentrations with height, both in observations and simulation. The simulated concentration increases vertically with a strong gradient between the first layer, homogeneously mixed, and the upper layers. The gradient across the PBL is even stronger over AMS (0.33 ppmv), which is located in the center of our estimated oceanic sink (see Fig. 3). In the real world the gradient in the first 1–2 km is probably smoother but the vertical resolution of the model is too coarse, and no dataset is available to constrain values across the PBL. For the upper layers above CGO, the baseline selection affects only weakly the annual concentration (around −0.05 ppmv at 4 km) in comparison to the larger effect, −0.2 ppmv, at the surface (not shown in Fig. 5). This fact suggests

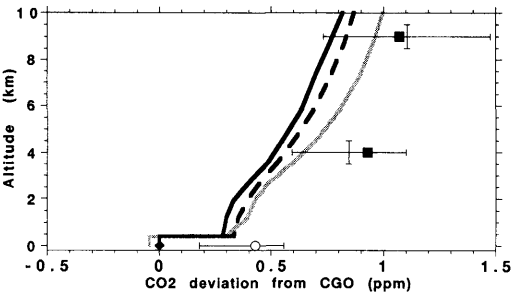

Fig. 5. Longitudinal and vertical annual gradients over Austral Indian ocean. Zero corresponds to CGO baseline values (black diamond). Observed values for the year 1990 are displayed for AMS (open circle) and mid-/high-troposphere (black squares). Horizontal error bars indicate the range value (±1 sigma) for the period 1988–1992. Vertical error bars indicate the range of the altitude of the flask sampling. Simulated profiles are shown by continuous curves: above AMS (gray line), and above CGO with (continuous line) and without (dashed line) baseline selection for upper layers.

that the sampling strategy, especially to deal with baseline conditions, during aircraft flight is not very sensitive. Another possible bias in the model/data comparison comes from the location of mid-troposphere sampling which extend from Bass Strait to over CGO, and can be affected by local gradient not simulated in the model. Recent data estimate this gradient around 0.1 ppmv (Francey, R., personal communication). For upper troposphere, this effect can be greater because aircraft flights was made above a wider area: the southern part of Australia.

Despite errors of the order of 0.2 ppmv due to the sampling strategy (see above) and the lack of continuous intercalibration (see part 2), our analysis brings out that the simulations failed, in a climatological sense, to match the data since: (1) the vertical gradient over CGO is too weak (around one third), though the gradient between mid and high troposphere is reasonably good, and (2) the longitudinal gradient AMS minus CGO is in opposite sign of the observations (AMS is estimated depleted relatively to CGO).

We have investigated how model/data discrepancies vary with the seasons. The monthly differences between CGO and AMS, and between CGO and the mid-troposphere are plotted in Fig. 6 (a and b). The low flight frequency (around once a month) forbids to resolve accurately the seasonal cycle with a few years dataset, so we have displayed

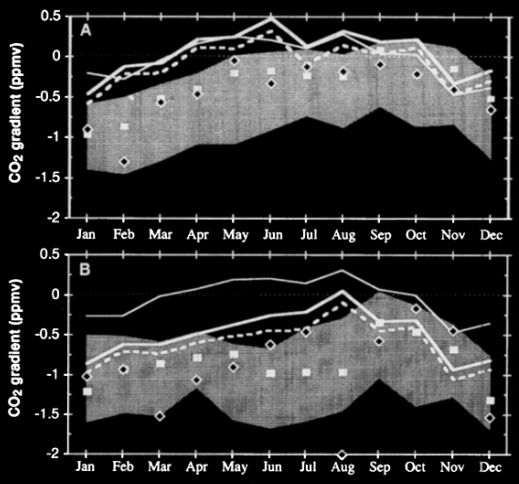

Fig. 6. Simulated and observed differences of CGO relative to AMS (a) and to the mid-troposphere (b). Data are as in Fig. 1, except standard deviations (shaded area) refer to 1980–1992 for (a) and to 1976–1992 for (b). Simulated values are displayed for 3 experiments: all components (thick line), only biospheric component (thin line) and all components with an extra oceanic sink (dashed thick line) (see text).

the standard deviation of monthly data averaged over a longer period (1980–1992 for CGO minus AMS; 1976–1992 for CGO minus aircraft measurements) than in Fig. 1. The lack of intercalibrations through the 1980–1992 period makes the annual difference between CGO and AMS (averaged over this period) poorly significant. However, this problem is less crucial for the shape of the seasonal cycle, because the drift of CO_2 scales probably occurs over few years, rather than few months. Finally, except in springtime (Sep–Nov), simulated differences between CGO and AMS are weaker than the observations, specially in Autumn (Mar–May). The seasonal cycle of the vertical gradient is correctly simulated for the first harmonic with larger gradients in summertime (Dec–Mar), as already pointed out by Tans et al. (1989), but not for the second harmonic with higher gradients during wintertime (Jun–Aug).

5. Discussions

As is shown in Fig. 5, the annual CO_2 concentrations over CGO decreases with height, both in the data and the model. Such a vertical gradient in the southern hemisphere may have two origins: (1) a drawdown of surface concentrations due to a surface sink, and (2) an enrichment of the upper troposphere due to CO_2-enriched air coming from the northern hemisphere. In the following, we discuss the contributions of the biospheric, industrial and oceanic components to the composite simulated gradients.

5.1. The continental biosphere

The terrestrial biospheric contribution dominates the composite seasonal cycle of atmospheric CO_2 in the southern hemisphere (Heimann et al., 1989; Ramonet, 1994). As illustrated by Fig. 6, the seasonal cycles of the differences of concentrations between (a) CGO and AMS, and (b) CGO and the mid-troposphere, are also mainly driven by the biospheric component.

In addition to seasonal variations, the terrestrial biospheric fluxes can also induce annual gradients according to two processes:

(a) An annual CO_2 sink or source. Yet, in southern middle latitudes the effect of deforestation or reforestation/fertilization is only of second importance for driving the annual mean CO_2 concentration (Heimann and Keeling, 1989; Ramonet, 1994). This is particularly true near Australia where biomass is located mainly on the East Coast.

(b) A cross-correlation between vertical mixing and CO_2 fluxes. As pointed out by Denning et al. (1995), although the net annual biospheric fluxes are equal to zero at every grid point (the NPP is balanced by the soil respiration over an annual cycle) they can induce annual mean gradients in the atmosphere. In fact, vertical stratifications are associated with CO_2 respiration (during night and/or wintertime). Consequently CO_2-enriched air is confined to the surface layer. On the other hand, strong convection occurs during the day and/or summertime, and dilute vertically the CO_2 depletion due to photosynthesis. This non-symmetrical process, during release or uptake of biospheric CO_2, enriches the annual mean concentrations in surface layer. This process can result in a 2 ppmv enhancement of the zonally averaged CO_2 concentrations in northern hemisphere (Denning et al., 1995; Rayner and Law, 1995). However, in southern hemisphere this effect seems

to be weaker by one order of magnitude (Rayner and Law, 1995).

Our model takes into account both processes "a" and "b". The seasonal variation of vertical mass flux due to cumulus convection is reproduced, but the coarse vertical resolution of TM2Z does not allow to reproduce the dynamic of the PBL. However, we have performed a sensitivity test which consists in expanding the continental PBL to two layers during summertime (the two first layers are homogeneously mixed), while in wintertime the first layer is vertically stratified according to the slope advection scheme used in the model (Russel and Lerner., 1981). The contribution of the terrestrial biosphere on annual vertical gradients at CGO and AMS is shown in Fig. 7. It is worth noting that the horizontal scale is different from Fig. 5. In any case the terrestrial biospheric contribution is weaker than 0.1 ppmv. Adding the baseline selection at CGO (not shown) results in an intermediate case between coastal case (CGO w/o selection) and marine case (AMS). The CGO minus AMS gradient is always weaker than 0.05 ppmv. So, a crude representation of the seasonal behavior of the continental PBL increases by only 0.05 ppmv the annual surface concentration at CGO. This is more than ten times less than the PBL effect in the northern hemisphere (Denning et al., 1995). Even if we reduce by a factor of two the vertical convection and diffusion, previous statements still remain true. In conclusion, the biospheric contribution appears to be too small to play a major role in the observed gradients.

5.2. *The fossil fuel CO_2*

A permanent CO_2 flow from the northern hemisphere to the southern hemisphere (resulting from the fossil fuel burning in industrial countries) had been highlighted by several authors (Pearman and Hyson, 1986; Keeling et al., 1989; Tans et al.; 1990). Rayner and Law (1995) had compared the simulation of this process by 12 atmospheric transport models. Basically, all the models produce in the southern hemisphere a mean depletion of the surface layer relative to the mid-troposphere (500 hPa), ranging from around 0.1 to 0.2 ppmv. This behavior is due to the preferential interhemispheric transport of CO_2-enriched air in the upper troposphere (see also Fig. 4, and Bousquet et al., 1996). The industrial contribution to the vertical gradients above CGO and AMS is shown on Fig. 8. As a sensitivity test, we have also plotted the gradients obtained with a reduced vertical mixing (convection and diffusion divided by a factor of two). Despite an uncertainty of a factor of 2 on the vertical gradient due to transport modeling (Rayner and Law, 1995), it clearly appears that a large scale fossil fuel structure cannot explain: (1) the observed CGO vertical gradient (around 1 ppmv throughout the troposphere); and (2) the surface depletion of CGO versus AMS (despite a

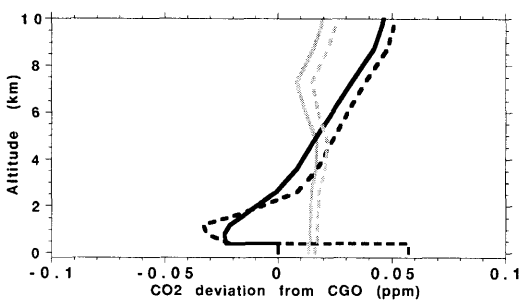

Fig. 7. Vertical annual gradients over Austral Indian ocean: the biospheric contribution. Black lines correspond to CGO (w/o selection), gray lines to AMS values. Two scenario are prescribed for PBL (see text): constant (continuous lines) or variable (dashed lines). All profiles are referred to CGO values with constant PBL.

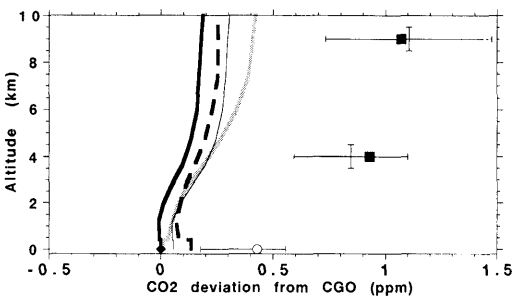

Fig. 8. Longitudinal and vertical annual gradients over the Austral Indian ocean: the fossil fuel contribution. Same as Fig. 6 but simulated profiles correspond only to fossil fuel CO_2: above AMS (gray line), and above CGO with (thick line) or without baseline selection (dashed line). Values are referred to CGO baseline value. The thin line is as thick line but corresponds to a sensitivity experiment where vertical convection and diffusion are divided by a factor of two.

0.2 ppmv difference in the upper troposphere). Finally, it is worth noting that the baseline selection at CGO removes a large part of the Australian industrial contribution (see Fig. 4), estimated around 0.15 ppmv in the surface layer and less than 0.1 ppmv in upper layers.

5.3. *The subtropical/subantarctic oceanic sink*

The contribution of oceanic sources/sinks to the vertical gradient above CGO and AMS is plotted in Fig. 9. Two main features appear: a first layer depleted by a few tenth of ppmv; and a regular decrease with height in upper layers. Such an oceanic component is strong enough to explain more than half of the observed vertical gradients. This is attributable to the fact that the subtropical/subantarctic ocean is the major CO_2 sink for the southern hemisphere. Near the surface a sharper gradient appears because AMS and CGO are located within the subtropical/subantarctic band where the CO_2 sink is located (see Fig. 2). This phenomena is stronger at AMS, located in the middle of the estimated sink (see Fig. 3).

Finally, our analysis indicates that the biospheric and industrial contributions are too small to explain the significant depletion of CGO compared to AMS and the mid-troposphere. The oceanic contribution seems to be the only one strong enough to explain the observed gradients. However, as shown above, our present estimation of the oceanic sink failed to match the observed gradients. Two problems in our simulations can be brought up to explain the disagreement: the crude representation of the PBL; and the estimation of the subtropical/subantarctic CO_2 sink. First, our representation of the PBL (400 m) in the TM2Z model minimizes the marine PBL, and so has a tendency to increase the vertical gradient over marine areas. Consequently, a more realistic marine PBL would not help to resolve the observed CGO depletion. Second, our estimation of the oceanic fluxes is based on oceanographic transects in the Atlantic ocean and the western part of the Southern Indian Ocean (see Fig. 2). As noted above, a large uncertainty remains on the global subtropical/subantarctic sink (1.4 ± 1 GtC y^{-1}). A 70% increase of this component (without rebalancing the whole oceanic budget) could explain the observed vertical gradient above CGO; but not the CGO depletion relative to AMS.

For this last reason, and also because the Australian continent can affect the oceanic circulation as well as the surface water characteristics (still unsampled for pCO_2), we have performed a sensitivity experiment, by adding an extra oceanic CO_2 sink off South Australia. Over an area of 20° in longitude by 10° in latitude south of Australia (126.25E to 146.25E/38.75S to 48.75S), we have depleted our estimation of ΔpCO_2 by -30 ppmv all around the year. This implies very low values of ΔpCO_2 all along the year in the considered oceanic region: -60 ppmv on annual average (from -80 ppmv in summer to -45 ppmv in winter), instead of -30 ppmv without the extra sink. Such an extra sink leads to improve the simulated annual gradients, in comparison to the observations (Fig. 10). But significant discrepancy remains as the Summer/Autumn depletion of CGO relative to AMS (Fig. 6), however no seasonal variability had been included in our sensitiv-

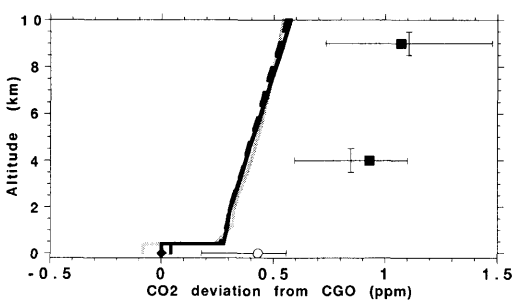

Fig. 9. Longitudinal and vertical annual gradients over Austral Indian ocean: the oceanic contribution. Same as Fig. 8 but simulated profiles correspond only to oceanic sources and sinks.

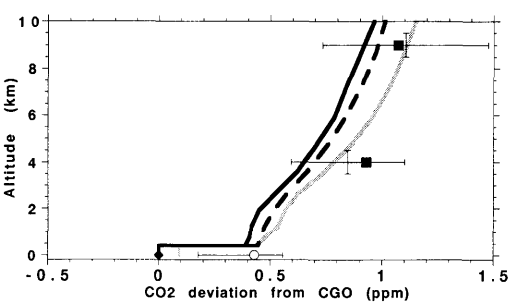

Fig. 10. Longitudinal and vertical annual gradients over Austral Indian ocean. Same as Fig. 5 but with an extra oceanic sink located south of Australia (see text).

ity experiment. Yet, it is worth noting that recent oceanographic campaign made by the CSIRO-Hobart in the region of interest reveal ΔpCO_2 as low as -80 ppmv during summertime (B. Tilbrook, personal communication). In spite of this confirmation of low ΔpCO_2, the strength of the hypothetical sink we deduce from our study remains poorly constrained because: (1) the area of such sink is not clearly defined, (2) the measured gradients can be affected by too low sampling frequency in the mid-troposphere and by systematic errors of the order of 0.2 ppmv (see above), and (3) the atmospheric transport modeling can also introduce systematic biases. However, our study clearly points out the interest of more oceanographic campaigns south of Australia to outline the regional and seasonal patterns of the CO_2 oceanic sink in this active area, and of an extended vertical CO_2 survey from Tasmania to Perth area.

6. Conclusions

We have focused our study on the East-West and vertical CO_2 gradients that exist over the southern middle latitudes, with the goal to relate them to the regional fluxes.

First, using the French–Australian CO_2 intercalibration (August 1990) and recent corrections for the drift of the Australian CO_2 calibration scale, we have found a permanent depletion of the Australian CO_2 monitoring station (Cape Grim, CGO) compared to the free troposphere (about 1 ppmv), and to Amsterdam Island (about 0.5 ppmv) which is located in the same latitudinal band.

Second, using a 3-D atmospheric transport model (TM2Z) based on meteorological analysis and on a global diagnostic scenario of CO_2 fluxes for the year 1990, we have analyzed the respective contributions of industrial, oceanic and terrestrial biospheric fluxes to the annual gradients. In contrast to the northern hemisphere, the influence of the terrestrial biosphere is small due to the lower continent/ocean area ratio in southern middle latitudes. This contribution is also lowered by the baseline selection which emphasizes the marine air masses. A sensitivity study was also performed to mimic the seasonal cross-correlation between biospheric fluxes and vertical mixing. It showed that in any case the terrestrial biosphere induces only small gradients (less than 0.1 ppmv) over the subtropical/subantarctic ocean.

The invasion of northern enriched-CO_2 air in southern hemisphere occurs preferentially in the upper troposphere, and it induces a relative depletion of surface layers in comparison to the mid-troposphere (of the order of 0.2 ppmv). Despite large uncertainties in the atmospheric transport modeling (about a factor of 2) we concluded that such a process explains only few tens per cent of the observed gradients.

The subtropical/subantarctic CO_2 oceanic sink appears to be the major process involved in the CGO depletion. Our present estimation of this oceanic sink is based on oceanographic campaigns made in the Indian, Atlantic and Pacific oceans. It is mainly located at the same latitude than CGO and AMS. Consequently, a few tenths of ppmv vertical gradient occurs throughout the PBL, together with a regular increase in the free troposphere of the same order of magnitude. Such an oceanic contribution explains more than half of the observed CO_2 gradient over CGO, but not the CGO depletion relative to AMS. Since our estimation of the oceanic sink, does not rely on any oceanographic observation from the eastern part of the Indian ocean, we have performed a sensitivity test by adding an extra oceanic sink south of the Australian mainland and west of Tasmania. With such an hypothetical CO_2 sink (ΔpCO_2 equal to -60 ppmv on annual average) it is possible to crudely reconstruct signs and magnitudes of both longitudinal and vertical gradients observed over the Southern Indian ocean. Furthermore, such a strong pCO_2 depletion in the water westward of Tasmania had been recently measured during summertime.

This agreement between our atmospheric prediction, of an oceanic CO_2 sink, and new oceanographic dataset is promising. The regional patterns of the oceanic fluxes may be successfully determined by aggregating both dense oceanographic and atmospheric datasets: one part used to establish a diagnostic of CO_2 fluxes, and the other part used as a validation tool.

However, the uncertainty of the measured gradient, around 0.2 ppmv, is still too large to precisely constrain the oceanic CO_2 sink near Australia. Further studies are also needed to estimate the role of the atmospheric boundary layer and of the vertical mixing, implying modeling and measure-

ments with higher resolution, both vertically, horizontally and seasonally. Particularly, study on the role of undersampling must be addressed versus flight frequencies. Finally, in a context of the changing climate and carbon cycle, both atmospheric and oceanic CO_2 monitoring stations are needed to determine the inter-annual variability of the southern oceanic sink.

7. Acknowledgments

The CO_2 data from the Baseline Air Pollution Station at Cape Grim, Tasmania, which have been used in this study, were supplied by D. J. Bearsdmore and G.I. Pearman of the CSIRO Division of Atmospheric Research, Australia. We acknowledge computing support from CEA/LMCE, and from CCVR/IDRIS. Our sincere thanks to Y. Balkanski, P. Bousquet, P. Ciais, A. Gaudry, B. Pak, R. Francey and P. Tans whose suggestions helped to improve the paper. This work is supported by the Programme National d'Etude de la Dynamique du Climat, and the Commission of European Community program Environment N° CEE EV5V CT92–0120. This is CFR contribution n°1815.

REFERENCES

Beardsmore, D. J. and Pearman, G. I. 1987. Atmospheric carbon dioxide measurements in the Australian region: data from surface observations. *Tellus* **39B**, 42–66.

Beardsmore, D. J. and Pearman, G. I. 1990. *Baseline carbon dioxide concentrations*, Baseline Atmospheric Program (Australia) 1988 (eds. S. R. Wilson and G. P. Ayers), Bureau of Meteorology, Melbourne.

Beardsmore, D. J. and Pearman, G. I. 1991. *Baseline carbon dioxide concentrations*, Baseline Atmospheric Program (Australia) 1989 (eds. S. R. Wilson and J. L. Gras), Bureau of Meteorology, Melbourne.

Beardsmore, D. J. and Pearman, G. I. 1992. *Baseline carbon dioxide concentrations*, Baseline Atmospheric Program (Australia) 1990 (eds. A. L. Dick and P. J. Fraser), Bureau of Meteorology, Melbourne.

Beardsmore, D. J. and Pearman, G. I. 1994. *Baseline carbon dioxide concentrations*, Baseline Atmospheric Program (Australia) 1991 (eds. A. L. Dick and P. J. Fraser), Bureau of Meteorology, Melbourne.

Beardsmore, D. J. and Pearman, G. I. 1995. *Baseline carbon dioxide concentrations*, Baseline Atmospheric Program (Australia) 1992 (eds. A. L. Dick and P. J. Fraser), Bureau of Meteorology, Melbourne.

Beardsmore, D. J., Pearman, G. I., de Silva, F. R. and Steele L. P. 1996. *The CSIRO (Australia) atmospheric carbon dioxide monitoring program by infra-red gas analysis: Post 1981 developments and data.* CSIRO Division of Atmospheric Research Technical Paper. in press.

Bousquet, P., Ciais, P., Monfray, P., Balkanski, Y., Ramonet, M. and Tans, P. 1996. Influence of two atmospheric transport models on inferring sources and sinks of atmospheric CO_2. *Tellus* **48B**, this issue.

Broecker, W. S., Ledwell, J. R., Takahashi, T., Weiss, R., Merlivat, L., Memery, L., Peng, T. H., Jahne, B. and Munich, K. O. 1986. Isotopic versus micrometeorologic ocean CO_2 fluxes: a serious conflict. *J. Geophys. Res.* **91**, 10517–10527.

Ciais, P., Tans, P. P., White, J. W. C., Trolier, M., Francey, R. J., Berry, J. A., Randall, D. R., Sellers, P. J., Collatz, J. G. and Schimel, D. S. 1995. Partitioning of ocean and land uptake of CO_2 as inferred by $\delta^{13}C$ measurements from the NOAA/CMDL global air sampling network. *J. Geophys. Res.* **100**, 5051–5070.

Conway, T. J., Tans, P. P., Waterman, L. S., Thoning, K. W., Kitzis, D. R., Masarie, K. A. and Zhang, N. 1994. Evidence for interannual variability of the carbon cycle from the National Oceanic and Atmospheric Administration/Climate Monitoring and Diagnostics Laboratory Global Air Sampling Network. *J. Geophys. Res.* **99**, 22831–22855.

Denning, A. S., Fung, I. Y. and Randall, D. A. 1995. Latitudinal gradient of atmospheric CO_2 due to seasonal exchange with land biota. *Nature* **376**, 240–243.

Enting, I. G. and Pearman, G. I. 1993. Average global distributions of CO_2. The Global Carbon Cycle, (ed. M. Heimann). *NATO ASI Series,* **I15**, 31–64.

Francey, R. J., Tans, P. P., Allison, C. E., Enting, I. G., White, J. W. C. and Trolier, M. 1995. Changes in oceanic and carbon uptake since 1982. *Nature* **373**, 326–330.

Fraser, P., Francey, R., Beardsmore, D., Coram, S., Goodman, H., Langenfelds, R. and Richards, N. G. 1992. *Cape Grim and Bass Strait aircraft overflights*, Baseline Atmospheric Program (Australia) 1990 (eds. A. L. Dick and P. J. Fraser) Bureau of Meteorology, Melbourne.

Gaudry, A., Monfray, P., Polian, G. and Lambert, G. 1987. The 1982–83 El-Ni–o: a 6 billion ton CO_2 release. *Tellus* **39B**, 209–213.

Gaudry, A., Monfray, P., Polian, G. and Lambert, G. 1990. Radon-calibrated emissions of CO_2 from South Africa. *Tellus* **42B**, 9–19.

Heimann, M. 1995. *The global atmospheric tracer model TM2.* Deutsches Klimarechenzentrum, Hamburg, Germany, Tech. Rep. 10, 51 p.

Heimann, M. and Keeling, C. D. 1989. A three dimensional transport model for atmospheric CO_2: (2)

Model description and simulated tracer experiments. *AGU Monograph* **55**, Washington, American Geophysical Union. 237–275.

Heimann, M., Keeling, C. D. and Tucker, C. J. 1989. A three dimensional transport model for atmospheric CO_2: (3) Seasonal cycle and synoptic time scale variations. *AGU Monograph* **55**, Washington, American Geophysical Union. 277–303.

Heimann, M., Monfray, P. and Polian, G. 1990. Modeling the long range transport of Rn-222 to subantarctic and antarctic areas. *Tellus* **42B**, 83–99.

Inoue, H. Y. and Sugimura, Y. 1988. Distributions and variations of oceanic carbon dioxide in the western North Pacific, eastern Indian, and Southern Ocean south of Australia. *Tellus* **40B**, 308–320.

Keeling, C. D., Piper, S. C. and Heimann, M. 1989. A three dimensional transport model for atmospheric CO_2 (4) Mean annual gradients and interannual variations. *AGU Monograph* **55**, Washington, American Geophysical Union. 305–363.

Keeling, C. D., Whorf, T. P., Wahlen, M. and Van Der Plicht, J. 1995. Inter-annual extremes in the rate of rise of atmospheric carbon dioxide since 1980. *Nature* **375**, 666–670.

Lambert, G., Monfray, P., Ardouin, B., Bonsang, B., Gaudry, A., Kazan, V. and Polian, G., 1995. Year-to-year changes in atmospheric CO_2. *Tellus* **47B**, 53–55.

Law, R. and Simmonds, I. 1996. The sensitivity of deduced CO_2 sources and sinks to variations in transport and imposed surface concentrations. *Tellus* **48**, in press.

Law, R. 1996. The selection of model-generated CO_2 data: a case study with seasonal biospheric sources. *Tellus* **48B**, this issue.

Liss, P. S. and Merlivat, L. 1986. *Air-sea gas exchange rates: introduction and synthesis. The role of air-sea exchange in geochemical cycling*, (ed. P. Buat-Menard). Adv. Sci. Inst. Ser., D. Reidel Pub. Co., 113–127.

Metzl, N., Beauverger, C., Brunet, C., Goyet, C. and Poisson, A. 1991. Surface water pCO_2 in the Western Indian sector of the southern ocean: a highly variable CO_2 source/sink region during the austral summer. *Mar. Chem.* **35**, 85–95.

Miller, J. M., Moody, J. L., Harris, J. M. and Gaudry, A. 1993. A 10-year trajectory flow climatology for Amsterdam Island, 1980–1989. *Atm. Env.* **27A**, 1909–1916.

Monfray, P., Ramonet, M., Gaudry, A., Pearman, G., Beardsmore, D., Manning, M. and Pohl, P. 1992. An intercalibration of CO_2 measurements between France, Australia and New Zealand. *WMO/GAW Report* **77**.

Pearman, G. I. and Beardsmore, D. J. 1984. Atmospheric carbon dioxide measurements in the Australian region: ten years of aircraft data. *Tellus* **36B**, 1–24.

Pearman, G. I. and Hyson, P. 1986. The global distribution of atmospheric carbon dioxide (1) Aspects of observations and modelling. *J. Geophys. Res.* **88**, 3581–3590.

Pearman, G. I., Beardsmore, D. J. and Francey, R. J. 1991. *Zonal representativeness of Cape Grim CO_2* measurements. CMDL, Summary Report 1990 (eds. E. E. Ferguson and R. M. Rosson), pp. 107–108.

Plumb, R. A. and Mahlman, J. D. 1987. The zonally averaged transport characteristics of the GFDL general circulation/transport model. *J. Atmos. Sci.* **44**, 298–327.

Poisson, A., Metzl, N., Brunet, C., Schauer, B., Bres, B., Ruiz-Pino D. and Louanchi, F. 1993. Variability of sources and sinks of CO_2 in the western Indian and Southern oceans during the year 1991. *J. Geophys. Res.* **98**, 22759–22778.

Prather, M., McElroy, M., Wofsy, S., Russel, G. and Rind, D. 1987. Chemistry of the global troposphere: Fluorocarbons as tracers of air motion. *J. Geophys. Res.* **92**, 6579–6613.

Rayner, P. J. and Law, R. M. 1995. *A comparison of modelled responses to prescribed CO_2* sources. CSIRO Div. Atmos. Res. Tech. Pap. 36/CRC Sthn. Hem. Meteor. Tech. Rep. 1, 82 p.

Ramonet, M. 1994. *Variabilité du CO_2* atmosphérique en régions australes: comparaison modèle-mesures. Thesis, University of Paris 7, 295 p.

Ramonet, M., Le Roulley, J. C., Bousquet, P. and Monfray, P. 1996. Radon-222 measurements during the TROPOZ II campaign and comparison with a global atmospheric transport model. *J. Atmos. Chem.* **23**, 107–136.

Ramonet, M. and Monfray, P. 1996. CO_2 Baseline concept in 3-D atmospheric transport models. *Tellus* **48B**, this issue.

Ruimy, A., Dedieu, G. and Saugier, B. 1994. Methodology for the estimation of terrestrial net primary production from remotely sensed data. *J. Geophys. Res.* **99**, 5263–5283.

Russel, G. L. and Lerner, J. A. 1981. A new finite-differencing scheme for the tracer transport equation. *J. Appl. Meteor.* **20**, 1483–1498.

Taguchi, S. 1993. Interhemispheric exchange in the troposphere by an atmospheric transport model based on observed winds. *J. Met. Soc. Jap.* **71**, 123–134.

Takahashi, T., Olafson, J., Goddard, J. G., Chipman, D. W. and Sutherland, S. C. 1993. Seasonal variation of CO_2 and nutrients in the high-latitude surface oceans: a comparative study. *Global Biogeo. Cycles* **7**, 843–878.

Tans, P. P., Conway, T. J. and Nakazawa, T. 1989. Latitudinal distribution of sources and sinks of atmospheric carbon dioxide derived from surface observations and an atmospheric transport model. *J. Geophys. Res.* **94**, 5151–5172.

Tans, P. P., Fung, I. Y. and Takahashi, T. 1990. Observational constraints on the global atmospheric CO_2 budget. *Science* **247**, 1431–1438.

Weiss, R. F., Van Woy, F. A. and Salameh, P. K. 1992. *Surface water and atmospheric carbon dioxide and nitrous oxide observations by shipboard automated gas chromatography: results from expeditions between 1977 and 1990.* Oak Ridge National Laboratory, USA: Carbon Dioxide Information Analysis Center, 616 p.